Droplets profiles and wetting transitions in electric fields

Marguerite Bienia[a,*], Frieder Mugele[b],
Catherine Quilliet[a], Patrice Ballet[a]

[a]*Laboratoire de Spectrométrie Physique, CNRS UMR 5588, Université Joseph Fourier, BP87, 140, avenue de la Physique, 38402 Saint-Martin-d'Hères Cedex, France*
[b]*Department of Applied Physics, University of Ulm, Albert-Einstein-Allee 11, 89081 Ulm, Germany*

Abstract

This paper presents current work in electrowetting. In the first part, we discuss experimental measurements of curvature of a conductive liquid drop in an electrical field. A recent theoretical and numerical study [8] predicts that diverging electric fields give rise to deviations close to the contact line from the usual spherical cap shape. We present here the first experimental measurements, compared to numerical simulations. In the second part, we recall how electrowetting is likely to induce wetting transitions, and describe the experimental setup designed to this purpose. Ellipsometry monitoring of film thickness is intended to follow total towards pseudo-partial wetting transition, allowing to reconstruct the effective interface potential of the system, acting like the electrostatic counterpart to the mechanical Surface Force Apparatus.
© 2004 Elsevier B.V. All rights reserved.

PACS: 68.08.Bc; 68.03.g; 47.65.+a; 68.05.n; 68.15.+e

Keywords: Wetting; Electrostatics; Liquid thin films

1. Introduction

The behavior of liquids in electrical fields is of fundamental and applied interest. Two effects can be outlined: dielectrophoresis [1]—for dielectric liquids—and electrowetting—for conductive ones. Electrowetting (EW) on an insulator-coated electrode consists in applying a voltage between a drop of conductive liquid and a counter electrode, separated by a thin dielectric layer. This results in a reduction of the contact

---

* Corresponding author.

E-mail address: mbienia@spectro.ujf-grenoble.fr (M. Bienia).

angle between the liquid and the solid [2]. This paper addresses two different topics related to electrowetting. The first is a fundamental study of the phenomenon itself, namely the shape of the drop near the three-phase line when a voltage is applied. The second, fundamental as well, deals with wetting transitions in water/oil/polymer systems, electrowetting being used as a trigger.

2. Experimental study of the curvature of a conductive liquid in electrical field

2.1. Introduction

Controlling the electrical field in order to tune either the wetting behavior of a surface or the shape of liquid micro-structures at high speed and with low-power consumption proved to be very efficient in many fields of applications such as micro-devices [3]. Nevertheless, fundamental research in EW is still vivid, in order to fully understand complex phenomena at the three-phase line such as contact angle saturation, which impedes complete wetting [4–6], and contact line instabilities [4,7], both occurring at high voltage. We will present fundamental investigation of the shape of a drop under electrical field in order to detect curvature changes due to electrostatic sharp edges effects. Such experiments may give some insight into fundamental questions such as droplet expulsion. Indeed, field-induced distortions of the interface profile may play a role in contact angle saturation and in particular in emission of small satellite droplets as the contact line becomes unstable [7]. The first results are compared with numerical simulations which predict a strong deviation of the curvature near the three-phase line.

2.2. Theory

Consider a drop of conductive liquid sitting on an insulating polymer solid, of relative dielectric constant ε_r and thickness d. An electrical voltage difference is applied between the drop and a counter electrode under the solid. The free energy of this system consists of two terms:

$$\mathscr{F} = \sum (\gamma_i A_i) - \tfrac{1}{2}\mathscr{C}V^2 \,, \tag{1}$$

with $\mathscr{C}$ the capacitance per unit area of the plane capacitor formed by the electrode and the liquid/solid interface [2]. The first term is the interfacial energy of the system, and the second is the electrostatic energy stored in the plane capacitor created by the counter-electrode and the liquid. This expression neglects sharp edge effects due to the finite size of the drop and to the sharp shape the drop takes at low contact angle. Vallet et al. [4] showed that the excess charge density σ diverged as a power function of the distance to the edge, assuming a wedged shape for the liquid. Knowing the electrical field and the shape of the drop simultaneously is a free boundaries problem that can be solved numerically. Buehrle et al. [8] performed self-consistent numerical calculations of drop profiles which show that the interface profile is indeed deformed near the three-phase line. They considered a drop of a perfectly conductive liquid, in
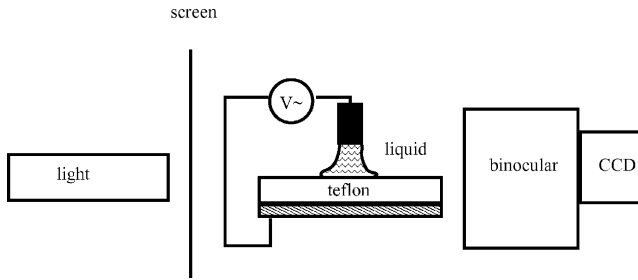
Fig. 1. Experimental setup. The screen is used to diffuse light. A wide electrode is used to trap the drop and prevent motion during the experiment.

2D. In mechanical equilibrium, the Maxwell stress, which the electric field exerts on the surface, is balanced locally by the capillary pressure:

$$P_{cap}(r) = P_{elec}(r) \, , \tag{2}$$

which leads to

$$\gamma\kappa(r) = \tfrac{1}{2}\varepsilon_0 E(r)^2 \, , \tag{3}$$

γ is the surface tension of the liquid, κ the mean curvature of the profile. A few iterative calculations of the electric field distribution $E(r)$ and the corresponding surface profiles lead to an equilibrium profile. They predict a deviation from the asymptotic curvature which occurs on a range of the order of magnitude of the thickness d of the insulator. The dielectric constant ε_r of the insulator must also be taken into account, so we expect to see a change on a range d/ε_r.

2.3. Experimental section

The samples consisted of sheets of thick Teflon ($d = 160$ or 500 μm). The liquid used was a 1:1 mixture of salt water (Na$_2$SO$_4$, 0.387 M, $d = 1.048$) and glycerol to reduce evaporation (resulting surface tension $\gamma_{liq/air} = 50$ mN m^{-1}). AC voltage at 1 kHz was applied in the range 1000–1500 V RMS. The drops, of typical volume of a few microlitres, were illuminated from the side using white light. Side pictures of the drops were acquired using a CCD video camera mounted on a binocular. The experimental setup is described in Fig. 1. Interface profiles were extracted from the pictures using a custom procedure written for Matlab. A sigmoidal fit is performed for a hundred points around the transition from white to black on every line of pixels in the bitmap file. The inflexion point of the fit is taken as the edge of the drop. Then, the mean curvature is calculated using box averages over 10 points in order to smoothen the results.

2.4. Results and discussion

Fig. 2 summarizes the results we obtained so far for a series of droplets on two different thicknesses and voltages. Experimental results are compared with simulations
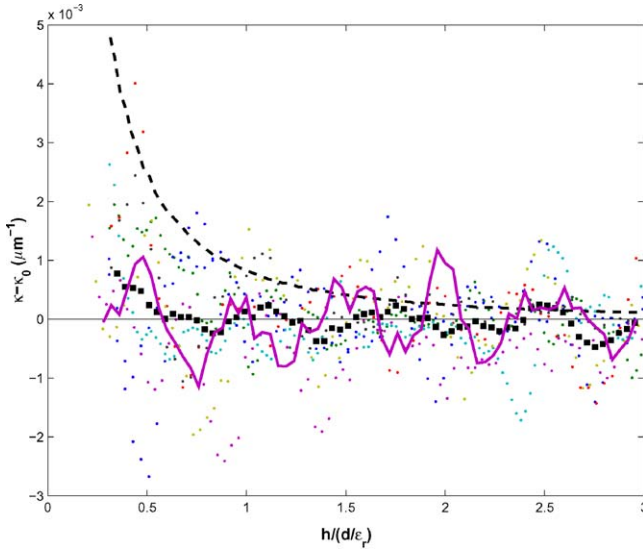
Fig. 2. Curvature deviation as a function of relative height. κ_0 is the macroscopic curvature. The solid line is the experimental result for 0 V, and dots are experimental results for two high voltages $V = 1000$ V and 1500 V. The squares represent the average of the data for $V \neq 0$. The dashed line is the simulation for $d = 100$ μm and $\varepsilon_r = 2$, at $V = 1000$ V.

using similar input parameters [8,9]. The results are rather noisy due to the two consecutive derivatives required for the curvature calculation. Therefore, we plotted all the results from a variety of different droplets together in one graph. In order to extract a qualitative trend, we plot the deviation of the local curvature from the macroscopic mean curvature $\kappa - \kappa_0$ versus the height above the substrate. The latter was normalized by d/ε_r. Despite the noise, a slight increase in curvature is apparent close to the substrate. Unfortunately, the data have to be truncated closer than ≈ 20 μm above the substrate due to the finite pixel size (1 px = 2.8 μm or 1 px = 5.8 μm depending on the experiments). These preliminary results are encouraging. However, further experiments, with thicker insulators and in particular with an improved optical setup are required in order to achieve more conclusive results.

3. Ellipsometric investigation of wetting transitions induced by electrowetting

3.1. Introduction

Wetting transitions are of fundamental interest in order to study long-range interactions between different media [10]. They also have interesting applications because they are involved in many industrial processes such as oil recovery or lubrication. We present here a new experimental setup designed to induce wetting transitions in a

water–oil–polymer system, using electrostatic interactions through the electrowetting (EW) effect.

With EW, contact angle reduction occurs until the system reaches saturation at a non-zero value of contact angle [4–7]. Since saturation prevents partial to complete wetting transitions of water on solid, we are interested in dewetting transitions, where the initial state is complete wetting for oil. A transition from complete wetting of oil on polymer will be triggered by the applied field between water and a counter-electrode beneath the polymer.

3.2. Theory of wetting transitions

Consider a system of oil and polymer solid in presence of water, in an EW geometry (i.e., potential difference applied between water and a counter electrode). Interactions between water and polymer across oil are described by the effective interface potential. The film energy per surface unit is $F(e)$ [11]:

$$F(e) = S + \frac{A}{12\pi e^2} - \frac{1}{2} \frac{\mathscr{C}_0 V^2}{(1 + \varepsilon_p e/\varepsilon d)} \,, \tag{4}$$

with A Hamaker constant of the solid–oil–water system [12], S wetting parameter [13], $e, \varepsilon, d, \varepsilon_p$, respectively, thickness and dielectric constant of oil and polymer, and $\mathscr{C}_0$ the capacitance of the system without oil. In the case of long-range repulsive interactions $(A > 0)$ and a positive wetting parameter S, the energy exhibits a minimum for a mesoscopic thickness of oil e_{eq} [11]:

$$e_{eq} = \left(\frac{\varepsilon_0 \varepsilon A}{3\pi \mathscr{C}_0^2 V^2} \right)^{1/3} . \tag{5}$$

The expected order of magnitude of e_{eq} is of a few nanometers for $V = 50$ V. For $V = 0$ V the system is in complete wetting. With increasing voltage, a transition towards "pseudo-partial" or frustrated wetting regime is induced, where a mesoscopic equilibrium thickness coexists with a thick reservoir. Up to now, such wetting transitions have only been obtained through temperature or pressure variation [14,15]. The oil thickness will be monitored by ellipsometry, allowing to probe the profile of the effective interface potential of the system.

3.3. Experimental section

The system used is Parylene C and bromododecane surrounded by sulfate brine. The sample consists of a silicon wafer, where the gold counter-electrode of 2000 Å in thickness is evaporated. A 2 μm layer of Parylene C is deposited in a CVD chamber in clean room conditions. The sample holder consists of two Teflon disks, one holding a toric joint, screwed together to ensure water-tightness, and forming a tank for the liquid. The top surface is open. The cell is described in Fig. 3.

We monitor oil thickness using a custom-made rotating birefringent ellipsometer where we implemented multilayer algorithms. Ellipsometry measures the ellipticity shift
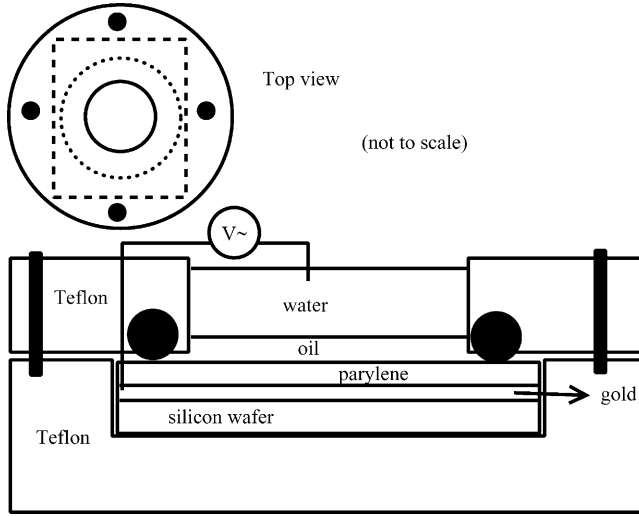
Fig. 3. Experimental cell.

of the incident laser beam through two parameters ψ and Δ:

$$\tan \psi \, \exp(\mathrm{i}\Delta) = \frac{R_p}{R_s} \, , \tag{6}$$

the subscripts p and s referring to parallel and perpendicular to the plane of incidence. Theoretical R_p and R_s are calculated using the matrix formalism developed by Azzam and Bashara [16]. The multilayer system we consider is oil-parylene, gold is the substrate and water is the ambient medium, with a correction due to non-normal incidence at the water/air interface. Indeed, the water layer is too thick for the multiple reflections at oil/water interface to interfere in a single beam. This results in several separated beams exiting the sample, giving several spots aligned vertically, as shown in Fig. 4. The top spot corresponds to reflection at the air/water interface. For the second spot, Eq. (7) is rewritten as follows:

$$\tan \psi \, \exp(\mathrm{i}\Delta) = \left(\frac{t_p}{t_s}\right)^{a/w} \left.\frac{R_p}{R_s}\right|_{multilayer} \left(\frac{t_p}{t_s}\right)^{w/a} \, , \tag{7}$$

t_p and t_s being the transmission coefficients for the water/air interface [17]. Either a silicon cell or a CCD video camera is used as a detector. The former allows quick measurements, whereas the latter allows to select the light spot to measure and can also perform ellipsometry imaging [18].

3.4. Conclusion

We presented the theoretical calculations that forecast the possibility of a wetting transition in electric field. We described the experimental setup of reflected beam

Fig. 4. Multilayer setup. When the second spot is selected, only oil and parylene are taken into account.

selecting ellipsometry that is currently developed in our group in order to investigate wetting transitions using electrostatic attraction as a trigger.

Acknowledgements

References

[1] T.B. Jones, M. Gunji, et al., J. Appl. Phys. 89 (2) (2001) 1441–1448.
[2] B. Berge, C.R.A.S. III 317 (1993) 157;
    C. Quilliet, B. Berge, Curr. Opin. Colloid Interface Sci. 6 (2001) 34.
[3] S.-K. Cho, H. Moon, et al., (2001). 2001 ASME International Mechanical Engineering Congress and Exposition: 207–213.
    R.A. Hayes, B.J. Feenstra, Nature 425 (2003) 383–385;
    M.G. Pollack, R.B. Fair, et al., Appl. Phys. Lett. 77 (11) (2000) 1725–1726;
    S. Yang, T.N. Krupenkin, et al., Adv. Mat. 15 (11) (2003) 940–943.
[4] M. Vallet, M. Vallade, et al., Eur. Phys. J. B 11 (4) (1999) 583–591.
[5] A. Quinn, R. Sedev, et al., J. Phys. Chem. B 107 (5) (2003) 1163–1169.
[6] H. Verheijen, M. Prins, Langmuir 15 (20) (1999) 6616–6620.
[7] F. Mugele, S. Herminghaus, Appl. Phys. Lett. 81 (12) (2002) 2303–2305.
[8] J. Buehrle, S. Herminghaus, et al., Phys. Rev. Lett. 91 (8) (2003).
[9] Juergen Buehrle, Private communication.
[10] F. Brochard-Wyart, J.M. Di Meglio, et al., Langmuir 7 (2) (1991) 335–338.
[11] C. Quilliet, B. Berge, Europhys. Lett. 60 (1) (2002) 99–105.
[12] J. Israelachvili, Intermolecular and Surface Forces, Academic Press, New York, 1985.
[13] P.-G. de Gennes, Rev. Mod. Phys. 57 (3, Part I) (1985) 827–863.

[14] K. Ragil, J. Meunier, et al., Phys. Rev. Lett. 77 (8) (1996) 1532–1535.
[15] E. Bertrand, H. Dobbs, et al., Phys. Rev. Lett. 85 (6) (2000) 1282–1285.
[16] R.M.A. Azzam, N.M. Bashara, Ellipsometry and Polarized Light, North-Holland, Amsterdam, 1975.
[17] M. Born, E. Wolf, Principles of Optics, Pergamon Press, New York, 1975.
[18] Beaglehole, Rev. Sci. Instrum. 59 (12) (1988) 2557–2559.